Montmorillonite face surface associated tris(bipyridine)chromium(3+) monitored electrochemically

ARTICLE *in* THE JOURNAL OF PHYSICAL CHEMISTRY · NOVEMBER 1988

Impact Factor: 2.78 · DOI: 10.1021/j100334a035

possible to achieve the same fitting with those three parameters by a strictly numerical procedure (e.g., nonlinear least-squares fitting by successive Gaussian linearizations).

The case of the Helmholtz layer capacitance (Figure 4d) as a fitting parameter is different. Large variations in that parameter cause only small distortions in the theoretical curve. Also, by comparison with the other Figure 4 and with eq 22, errors in that parameters will tend to mask errors in the others. It cannot be used as a fitting parameter.

The values of ϕ_i obtained with different type B samples vary between 0.2 and 0.4 V. The lower value of ϕ_i corresponds to a trap level at 1.7 eV and the higher to a trap level at 1.5 eV, both above the valence band edge (from eq 25). This is in agreement with the observed peak at those wavelengths in the sub-band-gap spectrum of these hematite samples.[9]

Conclusion

An exact model of a space charge layer containing monoenergetic deep traps, which includes the effect of the Helmholtz layer, can be used to extract from nonlinear Mott-Schottky data, in the limit of small ac frequencies, the carrier and trap concentrations as well as the ionization threshold potential.

A procedure was also suggested to test for the presence of an excessive concentration of surface states which would make that method inapplicable.

Acknowledgment. We thank Dr. A. H. Webster, Head, Physical Chemistry Section, for his support and technical proofreading of the manuscript and suggestions.

Registry No. Fe_2O_3, 1309-37-1; KOH, 1310-58-3; hematite, 1317-60-8.

Montmorillonite Face Surface Associated $Cr(bpy)_3^{3+}$ Monitored Electrochemically

Alanah Fitch,* Adina Lavy-Feder,† Samuel A. Lee, and Mary T. Kirsh

Department of Chemistry, Loyola University of Chicago, 6525 N. Sheridan Road, Chicago, Illinois 60626
(Received: September 4, 1987; In Final Form: May 3, 1988)

The assembly of $Cr(bpy)_3^{3+}$ (bpy = bipyridine) into montmorillonite face surface holes can be monitored at clay modified electrodes. Close packing onto the surface occurs after all charge sites are occupied. Close packing results in enantiomeric and valence selectivity. The diffusion coefficient for $Cr(bpy)_3^{3+}$ in montmorillonite is 7×10^{-12} cm^2/s. The partition coefficient into the clay is 9.4×10^3. Isopotential points in the cyclic voltammograms demonstrate a rate-limiting hole association of $Cr(bpy)_3^{3+}$.

Introduction

Montmorillonite clays are highly reactive plates. Each plate consists of a single Al octahedral layer sandwiched between two Si tetrahedral layers. The plate has two types of surfaces. There is a face surface, which is characterized by an array of hexagonal holes defined by the tetrahedral layer. There is an edge surface where the platelet has been broken (Figure 1). The two dimensionality of clays allows them to act as catalysts.[1]

Clays are ion-exchange materials. Negative charge arises due to isomorphous substitution of Mg^{2+} for Al^{3+} in the octahedral layer. This negative charge is experienced primarily between two platelets and is associated with the face surface. Edge bonds may be protonated or deprotonated. This results in a pH-dependent charge at edge sites. The magnitude of the pH-dependent edge charge is generally smaller than and independent of the fixed-site negative charge. Edge charge can be 20% of the total charge.[2] Due to the high charge of these clays there is enhanced acidity in the inner layer between two face surfaces. A number of unique organic catalysts have been prepared that make use of the high acidity of clays.[3]

The net negative charge of the clay results in electrostatic attraction of cations. Between two species of cations there is a competitive reaction for negatively charged sites on the clay. The overall ion-exchange reaction can be described in the following steps:[4]

$$AX_n^* \underset{k_{-1}}{\overset{k_1}{\rightleftharpoons}} AX_n^c \qquad (1)$$

$$AX_n^c + n(\text{Na-clay}) \underset{k_{-2}}{\overset{k_2}{\rightleftharpoons}} \text{A-clay} + n(NaX^c) \qquad (2)$$

where AX_n^* is the bulk solution ion-paired complex, AX_n^c and NaX^c are the ion-paired species in the vicinity of the face surface, Na-clay is the Na-exchanged clay, and A-clay is the complex-exchanged clay. The first step is a diffusion step, the rate of which depends on diffusion rate constant k_1, and the bulk solution concentration of the complex $[AX_n^*]$. The magnitude of k_1 depends on the spacing between plates. The second step is the ion-exchange step. The values of k_2 and k_{-2} depend on the charge of the clay, the relative charges on the cations, and, possibly, the extent of ion pairing. Ion pairing can be significant for complex cations such as the tris(diimine) studied here.[5] This kind of simple ion-exchange equilibrium at clays governs the uptake of many simple cations such as Ca^{2+}.[6]

In addition to electrostatic ion-exchange equilibria described above, other factors may govern uptake of cations by clay. From the work of Mortland,[7] Schoonheydt,[2] Fripiat,[8] and Yamagishi[9]

† Presently at Chemical Testing Laboratory, Technion, Haifa, Israel.

(1) (a) Montroll, E. W. *Proc. Symp. Appl. Math. Am. Math. Soc.* **1964**, *16*, 193. (b) Lazlo, P. *Science (Washington, D.C.)* **1987**, *235*, 1473.
(2) (a) Schoonheydt, R. A.; Pelgrims, J.; Heroes, Y.; Uytterhoeven, J.-B. *Clay Miner.* **1978**, *13*, 435. (b) Velghe, F.; Schoonheydt, R. A.; Uytterhoeven, J. B.; Peigneur, P.; Lunsford, J. H. *J. Phys. Chem.* **1977**, *81*, 1187.
(3) Krenske, D.; Abdo, S.; Van Damme, H.; Cruz, M.; Fripiat, J. J. *J. Phys. Chem.* **1980**, *84*, 2447.
(4) Sparks, D. L. In *Soil Physical Chemistry*; Sparks, D. L., Ed.; CRC Press: Boca Raton, FL, 1986.
(5) (a) Van Meten, F. M.; Newman, H. M. *J. Am. Chem. Soc.* **1976**, *98*, 1382. (b) Bizunok, M. B.; Pyatman, A. K.; Mironov, V. E. *Izv. Vyosh. Uchebn. Zaved., Khim. Khim. Tekhnol.* **1983**, *26*, 907.
(6) White, G. N.; Zelazny, L. W. In *Soil Physical Chemistry*; Sparks, D. L., Ed.; CRC Press: Boca Raton, FL, 1986.
(7) (a) Farmer, V. C.; Mortland, M. M. *J. Phys. Chem.* **1965**, *69*, 683. (b) Farner, V. C.; Mortland, M. M. *J. Chem. Soc. A* **1966**, 344. (c) Traynor, M. F.; Mortland, M. M.; Pinnavia, T. J. *Clays Clay Miner.* **1978**, *26*, 318. (d) Berkheiser, V. E.; Mortland, M. M. *Clays Clay Miner.* **1977**, *25*, 105.
(8) (a) Krenske, D.; Abdo, S.; Van Damme, H.; Cruz, M.; Fripiat, J. J. *J. Phys. Chem.* **1980**, *84*, 2447. (b) Abdo, S.; Canesson, P.; Cruz, M.; Fripiat, J. J.; Van Damme, H. *J. Phys. Chem.* **1981**, *85*, 797.
(9) (a) Yamagishi, A. *J. Phys. Chem.* **1982**, *86*, 2472. (b) Yamagishi, A. *J. Chem. Soc., Chem. Commun.* **1984**, 119. (c) Yamagishi, A.; Soma, M. *J. Am. Chem. Soc.* **1981**, *103*, 4640. (d) Yamagishi, A. *J. Chem. Soc., Dalton Trans.* **1983**, 679. (e) Yamagishi, A. *J. Am. Chem. Soc.* **1985**, *107*, 732. (f) Yamagishi, A. *Inorg. Chem.* **1983**, *21*, 3393.

0022-3654/88/2092-6665$01.50/0

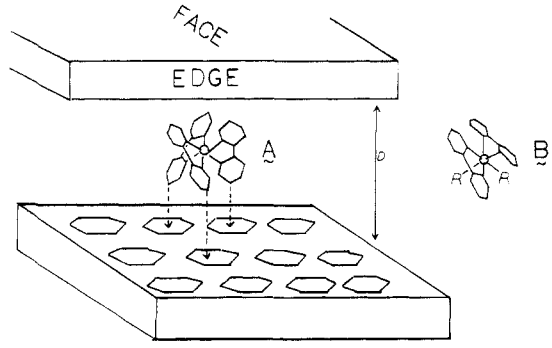

Figure 1. Idealized model of a face-to-face association of two clay platelets separated by the inner layer distance, D. The interaction of a tris(diimine) complex (A) with the face surface hexagonal holes is shown.

a model of surface-localized uptake of tris(diimine) complexes emerges (Figure 1). The unique equilateral triangular base of the trisdiimine complex (Figure 1A) matches the geometry of the hexagonal holes on the face surface of the clay.[9a] Both phenanthroline and bipyridine complexes have a geometry that matches the surface hole geometry. Complexes lacking this geometry (Figure 1B) will not match surface holes.

Docking of the complex begins at fixed negative charge sites as described by

$$\text{A–clay} \underset{k_{-3}}{\overset{k_3}{\rightleftharpoons}} \text{A–hole} \qquad (3)$$

Docking can then extend to any available site consisting of three hexagonal holes until full face surface (monolayer) coverage is achieved. Uptake in excess of a cation-exchange capacity (CEC) must be accompanied by an electrolyte anion. The anions SO_4^{2-} and Br^- allow uptake in excess of the CEC while Cl^- does not.[2,7c] Following monolayer coverage of the face surface additional layers of the complex can be adsorbed.[9f] This "excess" uptake is accompanied by expansion of the plate-to-plate distance (D in Figure 1).[10]

The model is subject to the following tests: (a) uptake should be dependent on geometry of the complex; (b) adsorption should be dependent upon the fixed-site charge of the clay; (c) a difference between negative-site saturation and surface saturation may exist; and as coverage of the face surface increases (d) steric hindrance and (e) Coulombic repulsion of neighboring complexes might be observed. Electrochemical techniques were chosen as a means of observing adsorption of the complex.[11] $Cr(bpy)_3^{3+}$ was chosen because of interest in possible photochemical uses.[12]

Materials and Methods

Reagents. $Ru(NH_3)_6Cl_3$ (Strem Chemicals, Newburyport, MA), $Fe(CN)_6K_3$ (Aldrich), and $Ru(bpy)_3Cl_3$ (Aldrich) were used as received. $Os(bpy)_3(PF_6)_2$,[13] $Cr(bpy)_3(ClO_4)_3$,[14] $Cr(bpy)_2(OH)_2ClO_4$,[15] and (−)-d-$[Cr(bpy)_3](PF_6)_3$[14] were synthesized by standard procedures. Based on the measured and reported specific standard rotations, the synthesized (−)-d-$Cr(bpy)_3^{3+}$ was 98% enantiomerically pure. $Cr(bpy)_2(H_2O)_2^{3+}$ was formed in place by photolysis of a solution of $Cr(bpy)_3^{3+}$. The conversion was monitored spectrophotometrically following the method of Maestri.[16]

Clays (SWY-1, STx-1, SHCa-1, and SAz-1, University of Missouri at Colombia, Department of Geology) were purified according to the method of Jackson.[17] Purified clay was resuspended in distilled water to form clay solutions of 2–25 g/L. Clay remained in suspension for several months. The cation-exchange capacity of the SWy-1 clay, as determined by exchange with Mg^{2+} followed by an EDTA titration of the Mg^{2+} displaced by Na^+ (0.74 mequiv/g), was in close agreement with the standard value for this source clay (0.76 mequiv/g).[18]

Clay Modified Electrode Preparation. The electrochemically active area of the Pt electrode was 5×10^{-3} cm^2. Three methods of preparation of clay modified electrodes were used. Method 1: Clays containing ≥0% of the CEC of $Cr(bpy)_3^{3+}$ were prepared and sonicated to redisperse the solution. Then a 1-μL solution of 5 g of clay/L was dried rapidly at 100 °C for 10 min followed by a 5-min cooling period. Method 2: Electrodes prepared as described in method 1 were cycled in solutions of $Cr(bpy)_3^{3+}$ until steady state was achieved (vide infra) and then dried as described for method 1. Method 3: the clay was preexchanged by addition of a complex into the clay suspension or by placing a clay modified electrode into a solution containing the desired concentration of the complex. These clay modified electrodes containing variable amounts of $Cr(bpy)_3^{3+}$ were dried in the dark for 12–48 h at room temperature.

Determination of Film Thickness. The clay film thicknesses, w, of electrodes prepared by method 1 were too thin to measure with a micrometer. The values of w measured with a micrometer for thicker films were correlated with the total mass of clay spread over a constant area. A linear relationship was found (correlation coefficient of 0.996). The value of w of an electrode prepared by method 1 was extrapolated to be 0.3 μm. This thickness is the minimum thickness of the film during the actual experiment as clays swell. The diffusion layer thickness, d, created during a cyclic voltammetric experiment (scan rate of 50 mV/s and a diffusion coefficient of 7×10^{-12} cm^2/s (vide infra)) was 0.15 μm. Films ≥0.3 μm in thickness gave identical results as would be predicted for $w > d$.

Instrumentation. An EGG PAR 273 potentiostat/galvanostat and an EGG PAR Model 0091 X–Y recorder were used to obtain cyclic voltammograms. Unless otherwise specified, scan rates of 50 mV/s were used for all experiments. Potentials were measured against the Ag/AgCl and saturated calomel electrodes (SCE). The electrode was held in N_2-purged electrolyte for 5 min, and a background scan taken, and then it was transferred to a 5-mL N_2-purged solution containing the complex. If the measured current remained constant over a period of 30 min to 1 h, a steady-state value was assigned. Steady-state cathodic peak heights (average relative standard deviation of 7%) were measured from the base-line current. Chronocoulometric experiments were performed as described by Anson.[19] Charge measured in the background was subtracted from the total charge measured.

Micrographs were obtained on a Pt electrode of a geometric surface area of 2×10^{-3} cm^2 with an Internal Scientific Instrument Model SX-30 scanning electron microscope. The electrodes were constructed by sealing 26-gauge Pt wire in a glass tube with a maximum length of 2 cm to allow for positioning. Micrographs were obtained on air-dried samples that had been previously

(10) (a) Cloos, P.; Laura, R. D.; Badot, C. *Clays Clay Miner.* **1975**, *23*, 417. (b) Farmer, V. C.; Mortland, M. M. *J. Phys. Chem.* **1965**, *69*, 683. (c) Farmer, V. C.; Mortland, M. M. *J. Chem. Soc. A* **1966**, 344. (d) Heller, L.; Yariv, S. *Isr. J. Chem.* **1970**, *8*, 391. (e) Cloos, P.; Laura, R. D. *Clays Clay Miner.* **1972**, *20*, 259.

(11) (a) Ege, D.; Ghosh, P. K.; White, J. R.; Equey, J. F.; Bard, A. J. *J. Am. Chem. Soc.* **1985**, *107*, 5644. (b) Liu, H. Y.; Anson, F. C. *J. Electroanal. Chem.* **1985**, *184*, 411.

(12) (a) Henry, M. S.; Hoffman, M. Z. *Adv. Chem. Ser.* **1978**, *168*, 91. (b) Henry, M. S. *J. Am. Chem. Soc.* **1977**, *99*, 6138. (c) Maestri, M.; Bolletta, F.; Moggis, L.; Balzini, V. *J. Chem. Soc., Chem. Commun.* **1977**, 491. (d) Bolleta, F.; Maestri, M.; Moggi, L.; Balzani, V. *J. Chem. Soc., Chem. Commun.* **1975**, 901. (e) Ballardini, R.; Varani, G.; Scandola, F.; Balzani, V. *J. Am. Chem. Soc.* **1976**, *98*, 7432. (f) Bolleta, F.; Maestri, M.; Balzani, B. *J. Phys. Chem.* **1976**, *80*, 2499. (g) Nijs, H.; Cruz, M. I.; Fripiat, J. J.; Van Damme, H. *J. Chem. Soc., Chem. Commun.* **1981**, 1026. (h) Nijs, H.; Cruz, M. I.; Fripiat, J. J.; Van Damme, H. *Nouv. J. Chim.* **1982**, *6*, 551. (i) Nijs, H.; Fripiat, J. J.; Van Damme, H. *J. Phys. Chem.* **1983**, *87*, 1279.

(13) Vining, W. E.; Caspar, J. V.; Meyer, T. J. *J. Phys. Chem.* **1985**, *89*, 1095.

(14) Kane-Maguire, N. A. P.; Hallock, J. S. *Inorg. Chim. Acta* **1979**, *35*, L309.

(15) Baker, B. R.; Mehta, B. *Dev. Inorg. Chem.* **1965**, *4*, 848.

(16) Maestri, M.; Bolletta, F.; Serpone, N.; Moggi, L.; Balzani, V. *Inorg. Chem.* **1976**, *15*, 2048.

(17) Mehra, O. P.; Jackson, M. L. *Clays and Clay Minerals, Proceedings of the 7th National Conference*; Swineford, A., Ed.; 1958.

(18) *The Data Handbook for Clay Materials and Other Non-Metallic Minerals*; Van Olphen, H., Ed.; Pergamon: New York, 1979, 19.

(19) Anson, F. C.; Ohsaka, T.; Savaent, J.-M. *J. Am. Chem. Soc.* **1983**, *105*, 4883.

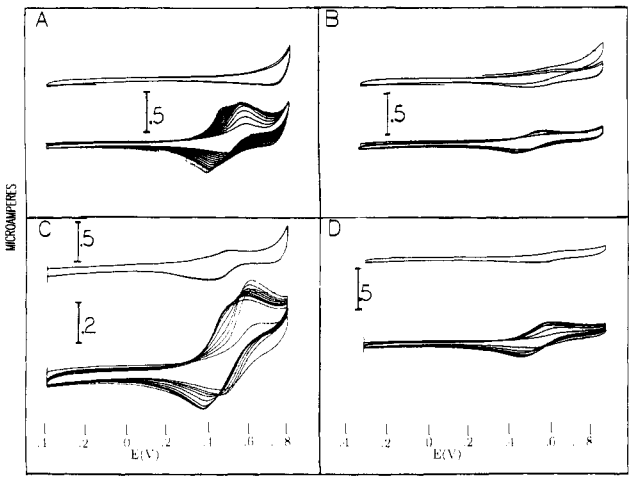

Figure 2. (A) Electrode preparation method 1 (see text); 27% preexchanged clay dried 10 min at 100 °C on Pt electrode. Cyclic voltammograms in 0.01 M Na_2SO_4 (upper) and in 0.19 mM $Cr(bpy)_3^{3+}$ (lower). (B) Electrode preparation method 2; electrode in A allowed to reach steady state, removed, and heated at 100 °C for 10 min. Cyclic voltammograms obtained in electrolyte (upper) and in 0.19 mM $Cr(bpy)_3^{3+}$ (lower). (C) Electrode preparation method 3; 160% preexchanged clay air-dried on Pt for 48 h (upper) and for 12 h (lower). Cyclic voltammograms obtained in 0.20 mM $Cr(bpy)_3^{3+}$. (D) Electrode preparation method 3; clay modified electrode allowed to reach steady state in 0.22 mM $Cr(bpy)_3^{3+}$ and then allowed to air dry 12 h. Cyclic voltammograms then obtained in electrolyte (upper) and in 0.22 mM $Cr(bpy)_3^{3+}$; potential vs SCE.

subjected to an electrochemical experiment and subsequently air dried.

Adsorption of $Cr(bpy)_3^{3+}$ and $Ru(bpy)_3^{2+}$ on clays were measured by a UV–vis spectrometer (Hewlett-Packard 8451A). Various amounts of the complex were added to 0.05 g of clay and brought to a total volume of 25 mL in either 0.01 or 0.1 M Na_2SO_4. The samples were equilibrated for 48 h, and the supernatant checked for remaining complex by measuring absorption at the $\pi-\pi^*$ lines (312 nm for $Cr(bpy)_3^{3+}$ and 288 nm for $Ru(bpy)_3^{2+}$).[20]

Results and Discussion

Clay Film Electroactivity as a Function of Preparation. Preparation of electrodes by method 1 yielded electrodes that readily took up the complex (Figure 2A). Peak heights at the modified electrode were larger than at the bare electrode, indicating concentration of the complex into the film. The presence of preexchanged material ≤100% CEC had little effect on the observed activity of the film. The film structure was unchanged from initial cycling in the electrolyte to steady state obtained with the complex present. No large pores were observed (Figure 3). Method 2 (Figure 2B) yielded electrodes with considerably lower electroactivity. Method 3 (Figure 2C,D) yielded electrodes whose electroactivity decreased as the evaporation time increased. Pinnavia[21] observed behavior similar to that of electrodes prepared by method 3.

These differences are attributed to clay structure effects as described by Derjaguin, Landau, Verwey, and Overbeek (DLVO) theory.[22] The equilibrium position of two charged plates is "flocculated" (face-to-face structure). A barrier to approach to this equilibrium position is due to the electrostatic repulsion of the two charged plates. If the double layer associated with the face surface is sufficiently compressed, the platelets are "shielded". The platelets may then approach in a face-to-face orientation close enough for attractive van der Waals forces to be felt. The activation energy controlling the rate of approach is governed by the ionic strength. Consequently the method of preparation and the electrolyte concentration used will affect the structure present during the cyclic voltammetric experiment. In preparation of the film, given sufficient time, clay platelets will orient to form films with stacked plates (face-to-face structure) whose c^* axis is perpendicular to the surface on which they are evaporated.[8a] In contrast, a clay gel solution that is freeze-dried retains its "aerogel" (edge-to-face or house of cards) structure.[23] In all subsequent measurements electrodes were prepared by method 1. In the cyclic voltammetric experiments, an electrolyte concentration of 0.01 M Na_2SO_4 was chosen to minimize face-to-face orientation.[24]

TABLE I: Maximum Height of the Reduction Peak Current for Face Associated $Cr(bpy)_3^{3+}$ Incorporated into Different Clays in 0.02 M NaCl

clay	CEC, mequiv/g	max i_p, μA
SAz-1	1.20	0.28
STx-1	0.85	0.20
SWy-1	0.764	0.13[a]
SHCa-1	0.44	0.08

[a] Maximum i_p for SWy-1 is less than in Figure 3 due to a change in electrode area (2×10^{-3} cm² here). Current densities are comparable.

Geometry of the Complex. Cyclic voltammograms of $Cr(bpy)_3^{3+}$ at clay modified electrodes showed a peak whose potential shifted to potentials more positive of those obtained at the bare electrode as uptake proceeded as indicated by increasing peak current (i_p; Figure 4A). When the electrode was transferred into a solution containing pure electrolyte, the peak currents decreased (material is lost from the electrode) and the potential of the peak shifted negative (Figure 4A). To determine if this peak is related to the docking of a tris(diimine) complex into surface holes, we investigated uptake of Ru and Os tris(bipyridine). Similar uptake patterns as Cr (i.e., a peak that shifts positive in potential as incorporation proceeds) were observed (Figure 4B,D).

Tris(diimine) complexes that have a bipyridine ligand removed lack the equilateral geometry necessary for interaction with the holes sites (Figure 1B). $Cr(bpy)_2(H_2O)_2^{3+}$ and $Cr(bpy)_2(OH)_2^{+}$ have a ligand removed. No uptake of $Cr(bpy)_2(OH)_2^{+}$ was observed. A reduction peak for $Cr(bpy)_2(H_2O)_2^{3+}$ was observed at the same potential as was observed for the complex at the bare electrode. No positive shifted peak occurred. $Ru(NH_3)_6^{3+}$ reduction peaks did not shift positive of the peaks obtained at the bare electrode either, even over a wide concentration range (0.02–1.0 mM). These results indicate that the shift toward more positive potentials upon incorporation depends on the geometry of the complex. This also shows that the shift toward more positive potentials is not due to the well-known lability of the $Cr(bpy)_3^{3+}$ complexes.[25]

Effect of the CEC on Uptake. Uptake was studied with respect to the measured CEC. The peak height of the positive shifted peak at steady state was measured from the base-line current and plotted as a function of the bulk solution concentration of the complex in 0.01 M Na_2SO_4[2+] and 0.02 M NaCl (Figure 5). Since uptake in the presence of Cl^- does not exceed the CEC,[7c] the observed limiting peak height (i_p = 0.32 μA) is associated with 100% saturation of charge sites. Limiting peak heights vary with the charge on the clay (Table I). This suggests that we are sampling the face surface associated complex.

To confirm the loading assignment, we measured the amount of material present after equilibration in 0.1 mM $Cr(bpy)_3^{3+}$. The electrode was transferred to the electrolyte solution, and the charge present measured by chronocoulometry. Background charge was subtracted, and the charge normalized for the electrochemically

(20) (a) Konig, E.; Herzog, S. *Inorg. Nucl. Chem.* **1970**, *32*, 585. (b) Inskeep, R. G.; Bjerrum, J. *Acta Chem. Scan.* **1961**, *15*, 62.
(21) King, R. D.; Nocera, D. G.; Pinnavia, T. J. *J. Electroanal. Chem.* **1987**, *236*, 43.
(22) Parker, J. C. In *Soil Physical Chemistry*; Sparks, D. L., Ed.; CRC Press: Boca Raton, FL, 1986.
(23) Van Olphen, H. *An Introduction to Clay Colloid Chemistry*, 2nd ed.; Wiley: New York, 1977; p 27.
(24) Fitch, A.; Fausto, C. L. *J. Electroanal. Chem.*, in press.
(25) (a) Zwickle, A. M.; Taube, H. *Discuss. Faraday Soc.* **1960**, *29*, 42. (b) Vleck, A. A. *Nature (London)* **1961**, *189*, 93. (c) Tucker, B. V.; Fitzgerald, J. M.; Hargis, L. G.; Rogers, L. B. *J. Electroanal. Chem.* **1967**, *13*, 400. (d) Soignet, D. M.; Hargis, L. G. *Inorg. Chem.* **1972**, *11*, 2921.

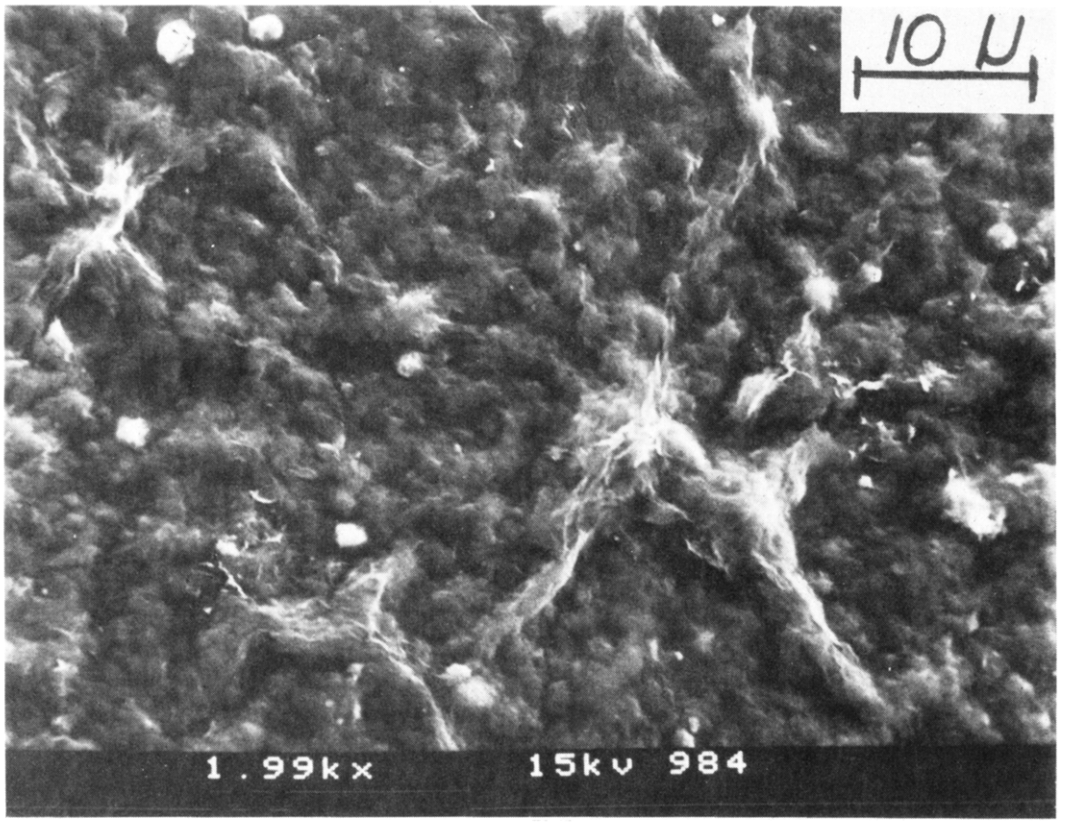

Figure 3. Scanning electron micrograph of clay modified electrode after steady-state cyclic voltammogram was obtained in 0.20 mM $Cr(bpy)_3^{3+}$ in 0.01 M Na_2SO_4. The bar is 10 μm.

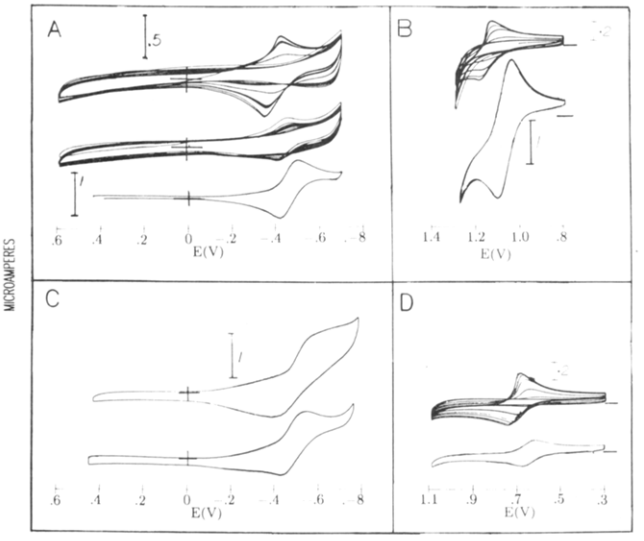

Figure 4. Cyclic voltammograms at clay modified and bare Pt electrodes; potential vs Ag/AgCl, 50 mV/s scan rates, electrolyte 0.01 M Na_2SO_4. (A) $Cr(bpy)_3^{3+}$. Upper: clay modified electrode in 0.1 mM complex with increasing peak heights measured at 4, 14, 27, 38, and 65 min. Curves coincident for 38 and 65 min. Middle: transfer of the electrode described in the upper panel to electrolyte showing decreasing peak heights on continuous scanning. Lower: bare Pt in 0.48 mM complex. (B) $Ru(bpy)_3^{2+}$. Upper: clay electrode in 0.2 mM complex with increasing peak heights measured at 1, 36, 54, 69, and 104 min. Lower: bare Pt electrode in 1.5 mM complex. (C) $Cr(bpy)_2(H_2O)_2^{3+}$; clay modified electrode (upper) and Pt electrode (lower) in 0.49 mM complex. (D) $Os(bpy)_3^{2+}$. Upper: clay modified electrode in 0.2 mM complex with increasing peak heights measured at 1, 16, 35, 51, 64, and 94 min. Lower: bare Pt electrode in 0.2 mM complex.

active area of the Pt electrode as a fraction of the total clay film area. The number of moles present was found to be 1.21×10^{-9}. This number of moles is due to the total material present, C_T:

$$C_T = [AX_n^c] + [A\text{–clay}] + [A\text{–hole}] \quad (4)$$

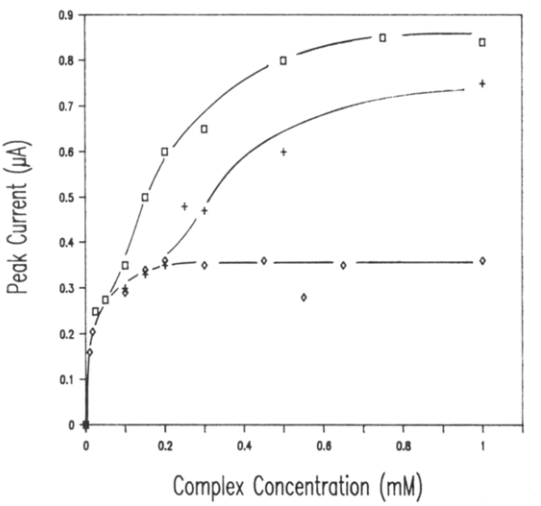

Figure 5. Cathodic peak height of positive shifted peak (couple I) as a function of complex bulk solution concentration: (□) racemic $Cr(bpy)_3^{3+}$ in 0.01 M Na_2SO_4; (+) (−)*d*-$[Cr(bpy)_3](PF_6)_3$ in 0.01 M Na_2SO_4; (◇) racemic $Cr(bpy)_3^{3+}$ in 0.02 M NaCl.

At equilibrium $[AX_n^c] = [AX_n^*]$. Even assuming that 50% of the clay film is pore space, the total number of moles of complex present as $[AX_n^c]$ can be no more than the product of the film volume, the bulk concentration, and the porosity. This value is 1.5×10^{-14} mol. Therefore the first term in eq 4 is dropped. The value of C_T should be determined by the CEC since the peak height measured (0.3 μA) was near the limiting value attributed to the CEC. The number of moles of trivalent complex predicted to be present in response to the CEC was 1.28×10^{-9} moles, showing excellent agreement with the measured value. This confirms that the uptake curves are close reflections of uptake in response to the cation-exchange capacity.

Monolayer Adsorption on the Face Surface. The extent of uptake at monolayer surface coverage as compared to coverage at 100% of the CEC can be predicted. From the elemental analysis

of SWy-1 (ref 18) and with the assumption that all charge arises from substitution of Mg^{2+} for Al^{3+} in the octahedral layer, the number of holes per charge can be calculated to be 6.9. At 100% of the CEC for SWy-1, a trivalent complex electrostatically "occupies" 21 (3 × 6.9) holes on a single plate, or 10.5 (21/2) holes for a complex located between two stacked platelets. At *monolayer* coverage each complex occupies 3 holes per complex (Figure 1), which is a 7- or 3-fold increase in concentration for a single vs dual plate association. Ion-paired complexes must be intercalated to achieve full surface coverage. The maximum cathodic peak height in SO_4^{2-} (0.85 μA) exceeds that obtained in Cl^- (0.32 μA) by a factor of 2.6 (Figure 5). If there is no large change in the apparent diffusion coefficient, this change in peak height agrees well with the predicted increase in incorporated material. No uptake in excess of the CEC occurs in Cl^-.[7c]

Transfer of the clay modified electrode preequilibrated in the complex solution to the electrolyte solution should result in peak heights corresponding only to the strongly (not ion paired) retained material (i.e., amount equivalent to CEC). Peak heights decreased by 30–60% on transfer to the electrolyte on the first scan. This decrease is due to loss of ion-paired complex. The peak height of the remaining complex was found to have a linear relationship with the bulk solution concentration used for equilibration (correlation coefficient = 0.94), the intercept of the line equal to 0.25 μA. This peak height roughly corresponds to the maximum peak height in the presence of Cl^- and is attributed to the more highly selective retention of the complex in response to the CEC.

Enantioselectivity. The docking model of uptake (Figure 1) predicts enantioselective uptake. At 100% loading of the CEC, the packing model suggests either 10.5 or 21 holes/complex, for a dual and single plate association, respectively. For 9 holes/complex a metal center to metal center distance of approximately 17 Å can be predicted. For this and larger spacings, steric constraints will not be evident. The monlayer (close packed) film (3 holes/complex) will result in a metal center to metal center distance of 8.25 Å. When the complex is oriented with its C_3 axis nearly perpendicular to the surface,[9a] the pseudo-C_4 axis is at a 45° angle from the surface. The C_3 axis of $Fe(phen)_3^{2+}$ (phen = phenanthroline) is 9 Å, and therefore a projection of the pseudo-C_4 axis to the surface yields a surface diameter of 9 Å. The interpenetration of ligands would be 9 − 8.25, or 0.75, Å.

Steric hindrance can be probed by varying the ligand size or by observing uptake from racemic vs enantiomeric solutions of the tris(bipyridine) complex. It is easier to pack complexes by alternating the enantiomers (*d*, *l*, *d*, *l*, etc.) as opposed to a single enantiomer (*d*, *d*, *d*, or *l*, *l*, *l*, etc.).[9a] This packing model is confirmed by molecular modeling using MNDO methods.[26] The cathodic peak current height vs bulk solution concentration in (−)*d*-$[Cr(bpy)_3^{3+}]$ is shown in Figure 5. Larger cathodic peak current heights are obtained from the racemic than from the enantiomeric solution once the CEC is exceeded.

Valence Selectivity: Relative Stability of M^{2+} vs M^{3+} Complexes. As packing density increases, repulsive interaction increases leading to selectivity for the lower valence complex. Neglecting all other differences in uptake for the different species, a positive shift in potential will result as illustrated by the following square scheme:

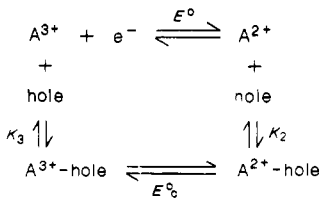

From which we find

$$E^0_c - E^0 = (RT/nF) \ln (K_2/K_3) \quad (5)$$

A positive shift in potentials is observed (Figure 6A). This shift does not prove that valence selectivity operates since oxidation/reduction potentials in films are also dependent on ion flux.[27] Confirmation of valence selectivity was obtained by noting the displacement of $Cr(bpy)_3^{3+}$ by $Ru(bpy)_3^{2+}$, but not of $Ru(bpy)_3^{2+}$ by $Cr(bpy)_3^{3+}$. An electrode reaching steady state in 0.1 mM $Cr(bpy)_3^{3+}$ solution showed a decrease in the cathodic peak current height of the positively shifted $Cr(bpy)_3^{3+}$ couple and an increase in the positively shifted $Ru(bpy)_3^{2+}$ couple when the solution was made 0.1 mM in both $Cr(bpy)_3^{3+}$ and $Ru(bpy)_3^{2+}$. The converse was not true.

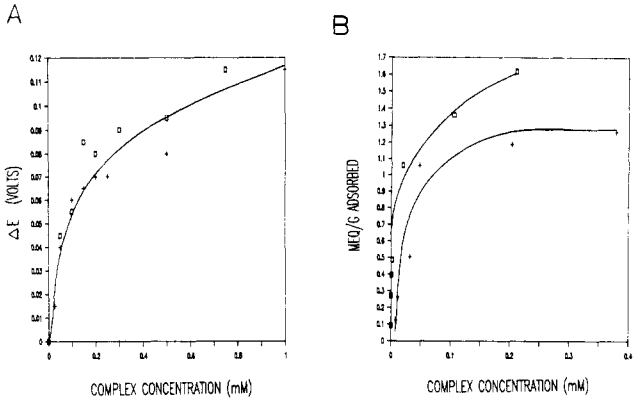

Figure 6. (A) Plot of $E^0_{clay} - E^0_{soln}$ (ΔE^0) vs the bulk solution concentration of $Cr(bpy)_3^{3+}$ for two Na_2SO_4 concentrations: (□) 0.01 M and (+) 0.1 M. (B) $Cr(bpy)_3^{3+}$ (+) and $Ru(bpy)_3^{2+}$ (□) uptake by SWy-1 from 0.01 M Na_2SO_4 as a function of equilibrium bulk solution concentration measured by UV–vis absorption.

Selectivity was additionally demonstrated by the uptake curves for $Ru(bpy)_3^{2+}$ and $Cr(bpy)_3^{3+}$ (Figure 6B). $Ru(bpy)_3^{2+}$ was removed more efficiently from solution at low bulk solution concentrations. Complete removal from solution has been observed elsewhere.[2,7-9] The number of clay sites exchanged was greater in $Ru(bpy)_3^{2+}$ than in $Cr(bpy)_3^{3+}$ at any bulk solution concentration.

The partition coefficient can be measured from the straight-line portion of the uptake curve before saturation of sites occurs. The partition coefficient,[28] α (C_{film}/C_{soln}), for $Cr(bpy)_3^{3+}$ was found to be 1.6×10^4 mequiv/(g M) or, with the moist bulk density for a conversion factor, 9.4×10^3. This coefficient is of the correct order of magnitude for the data obtained from the chronocoulometric experiments, 4.4×10^3. The partition coefficient for $Ru(bpy)_3^{2+}$, obtained by spectroscopy, was 2.1×10^5. The ratio of partition coefficients of $Ru(bpy)_3^{2+}$ to $Cr(bpy)_3^{3+}$ (α_2/α_3) is 22.

Rate of the Hole Association Step. For $Cr(bpy)_3^{3+}$, the growth of only a single peak, I (A–hole), is observed when $[AX_n^*]$ is small (Figure 4A), indicating that the rate-determining step is reaction 1. When $[AX_n^*]$ is large (Figure 7), the rate of reaction 1 is fast and either reaction 2 or 3 is rate limiting. Since an isopotential point[29] is observed, we conclude that step 3 is rate limiting. The isopotential point implies that the total material is distributed between A–hole and A–clay and that the magnitude of [A–clay] vs [A–hole] varies with time:

$$C_T = [\text{A–clay}] + [\text{A–hole}] \quad (6)$$

$$d[\text{A–hole}]/dt = k_3[\text{A–clay}] \quad (7)$$

Since the equilibrium constant for the hole association is large, quantitative uptake eventually results[2,5-7] and C_T becomes equal

(26) Lipkowitz, K., personal communication.

(27) Naelgeli, R.; Redepenning, J.; Anson, F. C. *J. Phys. Chem.* **1986**, *90*, 6227.

(28) (a) White, H. S.; Leddy, J.; Bard, A. J. *J. Am. Chem. Soc.* **1982**, *104*, 4811. (b) Szentirmay, M. N.; Martin, C. R. *Anal. Chem.* **1984**, *56*, 1898.

(29) (a) Untereker, D. F.; Bruckenstein, S. *Anal. Chem.* **1972**, *44*, 1009. (b) Cadle, S. H.; Bruckenstein, S. *Anal. Chem.* **1972**, *44*, 1993. (c) Untereker, D. F.; Bruckenstein, S. *J. Electroanal. Chem.* **1974**, *57*, 77. Cadle, S. H. *Anal. Chem.* **1974**, *46*, 587. (d) Chagas, H. C. *Can. J. Chem.* **1979**, *57*, 2560. (e) Abruna, H. D.; Walsh, J. L.; Meyer, T. J.; Murray, R. W. *Inorg. Chem.* **1981**, *20*, 1481. (f) Shigehara, K.; Oyama, N.; Anson, F. C. *J. Am. Chem. Soc.* **1981**, *103*, 2552.

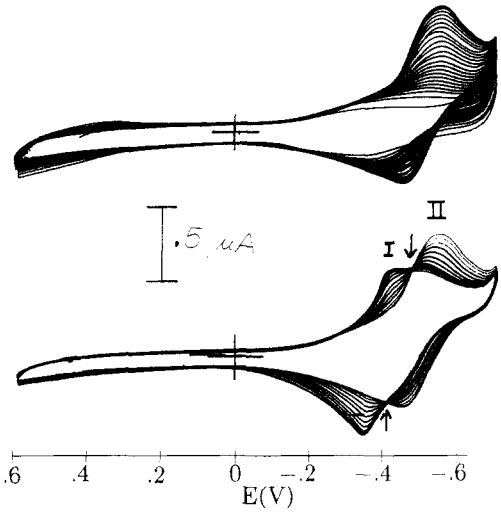

Figure 7. Cyclic voltammogram obtained in 0.15 mM $Cr(bpy)_3^{3+}$ in 0.01 M Na_2SO_4 where the isopotential point (arrow) is well developed. The two groups represent a continuous series of measurements in which couple II first increases in peak height (upper) and then decreases as couple I increases (lower); potential is vs Ag/AgCl.

to [A–hole]. C_T was determined by measuring $[A–hole]_{t=40min}$ chronocoulometrically and calculating the concentration by using the moist bulk density of the clay (1.77 g/cm^3).[30] The value of $[A–hole]_t$ at any time t during incorporation can be determined from the peak height of couple I:

$$[A–hole]_t = i_{pI(t)}/(2.69 \times 10^5)n^{3/2}AD_{app}^{1/2}v^{1/2} \quad (8)$$

where i_{pI} is the height of peak I in amperes, A is the electrochemically active area of the Pt electrode in cm^2, D_{app} is the apparent diffusion coefficient of A–hole in cm^2/s, v is the scan rate in V/s, and n is the number of electrons transferred.[31] D_{app} was measured by a plot of peak height in the electrolyte vs $v^{1/2}$. The plot resulted in a straight line (correlation coefficient of 0.999) from which the diffusion coefficient was found to be 7×10^{-12} cm^2/s, which compares reasonably well with $Os(bpy)_3^{2+}$ (1.2×10^{-12} cm^2/s) within clays.[11a]

With eq 6–8 and the peak heights in Figure 7, an estimate of k_3 was found to be 10^{-3} s^{-1}. No rate of packing was measurable for $Ru(bpy)_3^{2+}$ as no isopotential points were observable at any concentrations in 0.01 M Na_2SO_4. This means that k_3 for $Ru(bpy)_3^{2+}$ is much faster than k_3 for $Cr(bpy)_3^{3+}$. A very high packing rate (18 s^{-1}) has been observed for the $Fe(phen)_3^{2+}$ complex on clay.[9a] This difference in packing rate is consistent with valence selectivity in packing of the tris(diimine) complexes onto face surface holes on montmorillonite.

Further work is in progress to elucidate the various rate controlling steps as the experimental conditions (bulk solution complex concentration, Na^+ concentration, drying conditions, solvent, and temperature) are varied.

Summary

The uptake of diimine complexes into clays has been studied by electrochemical techniques. The electroactivity depends on the method of preparation. The bipyridine complexes are face surface adsorbed in a nonelectrostatic manner due to geometric considerations. The partition coefficient from solution into the clay for $Cr(bpy)_3^{3+}$ is 9.4×10^3. The rate constant for the formation of the hole associated species is 10^{-3} s^{-1}. The diffusion coefficient of $Cr(bpy)_3^{3+}$ in montmorillonite is 7×10^{-12} cm^2/s. Enantiomeric selectivity was observed. These results indicate that a method is available for the very precise spacing of the redox couple onto the face surface of the clay and that the chemical environment in the inner layer of the clay can be probed sensitively by electrochemical means.

Acknowledgment. Our thanks to J.W. Stuckey, Department of Agronomy, University of Illinois, Urbana, and J. Leddy, Queens College, CUNY, for informative discussions, to J. Hupp, Northwestern University, for the gift of $Os(bpy)_3^{2+}$, to K. Lipkowitz, Purdue University at Indianapolis, for computer modeling, and to the reviewers for their helpful comments. A.L.-F. was supported by a G.D. Searle postdoctoral fellowship. This work was also supported by a Loyola University of Chicago Summer Research Grants and NSF Grant Chem8707710.

Registry No. $Cr(bpy)_3^{3+}$, 15276-15-0; $Ru(bpy)_3^{3+}$, 15158-62-0; Pt, 7440-06-4; (−)-*d*-$[Cr(bpy)_3](PF_6)_3$, 41707-04-4; NaCl, 7647-14-5; Na_2SO_4, 7757-82-6; $Cr(bpy)_2(H_2O)_2^{3+}$, 36513-26-5; $Os(bpy)_3^{2+}$, 23648-06-8; montmorillonite, 1318-93-0.

(30) Grim, R. H. *Clay Mineralogy*; McGraw-Hill: New York, 1968; p 465.

(31) Bard, A. J.; Faulkner, L. R. *Electrochemical Methods*: Wiley: New York, 1980; p 218.